

Real-Time, Ultrasensitive Detection of RDX Vapors Using Conjugated Network Polymer Thin Films

Deepti Gopalakrishnan and William R. Dichtel*

Department of Chemistry and Chemical Biology, Cornell University, Baker Laboratory, Ithaca, New York 14853-1301, United States

S Supporting Information

1,3,5-Trinitro-1,3,5-triazine (RDX) and octahydro-1,3,5,7-tetra-nitro-1,3,5,7-tetrazocine (HMX) are low volatility explosives that are used in improvised explosive devices (IEDs) and employed in acts of terrorism. Standoff explosive detection depends on sensing these agents, their degradation products, or volatile contaminants, at subequilibrium vapor pressures (<6 parts per trillion for RDX). Analytical techniques that have been applied for trace RDX sensing include colorimetric immunoassays,^{1,2} surface-enhanced Raman spectroscopy,^{3,4} ion mobility spectroscopy,⁵ and changes in the surface plasmon resonance of Au nanoparticles.^{6,7} Many of these techniques require specialized equipment and/or preconcentration strategies^{1,8–15} that detract from their applicability.

The quenching of mobile excitons within conjugated polymer thin films provides signal amplification, which has been used for the ultrasensitive detection of TNT and other analytes.^{16,17} RDX has been detected directly from solution¹⁸ or indirectly from the vapor phase through covalent modification that provided a turn-on fluorescence response¹⁰ or by sensing volatile materials associated with RDX synthesis.¹⁹ More recently, high surface area materials, such as metal organic frameworks (MOFs),^{20,21} conjugated microporous polymers,²² and noncovalent assemblies of conjugated macrocycles²³ have been explored for detecting explosives, motivated in part by the possibility of combining preconcentration and sensing functions. Recently, we reported a polymer network, tris-(phenylene)vinylene (TPV), whose fluorescence was quenched by RDX introduced from solution and from the vapor phase.²⁴ Its high sensitivity represented an improvement over previous systems, which responded to RDX vapors over hours.²⁵ Nevertheless, several important parameters of the TPV films that impact sensing performance could not be controlled because the TPV network is inherently insoluble and precipitated from the reaction mixture onto included substrates. This process provided nonuniform films of uncontrolled thickness and precluded the use of nonplanar substrates, such as narrow capillaries used by commercial explosives detectors. Here we achieve consistent and robust TPV films by conducting the polymerization in the presence of fused SiO₂ substrates bearing allyl-siloxane monolayers (Figure 1). Surface-bound alkenes react with styrenic alkenes of the monomer to bond the network to the substrate. This approach yields continuous and consistent films, which provided control of the film thickness and extent of the metathesis reaction by varying the initial monomer concentration and reaction time. With this improved control, the sensitivity of the film, as well as its response time, were evaluated using both static and real-time fluorescence quenching experiments by introducing RDX from

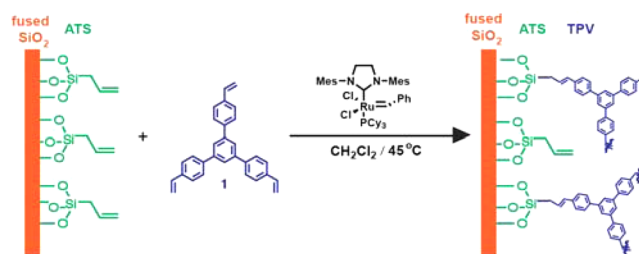


Figure 1. Schematic of TPV polymerization on allylsilane-functionalized fused SiO₂ substrates.

the solution or vapor phase. These optimized TPV films displayed a measurable response to RDX vapor in as little as 10 s, as well as to attogram amounts of HMX introduced from solution, making these polymer films of interest for security applications.

Fused SiO₂ substrates bearing TPV network films were prepared by performing acyclic diene metathesis (ADMET) polymerization of monomer **1** in the presence of fused SiO₂ substrates modified with an allylsilane monolayer (Figure 1). The TPV films exhibit UV/vis absorption profiles with absorbance at $\lambda_{\text{max}} = 280$ nm, corresponding to styrenic vinyl groups, and at $\lambda_{\text{max}} = 350$ nm, corresponding to newly formed stilbene chromophores (Figure 2A). The ratio of these peaks provides a qualitative sense of the extent of metathesis reaction. In our previous study thick films with more intense absorbance at $\lambda_{\text{max}} = 350$ nm relative to that at $\lambda_{\text{max}} = 280$ nm were the most sensitive to RDX. These films had been synthesized at relatively high initial monomer concentration ($[1]_0 = 70$ mM) for long reaction times (72 h) and were quite thick (optical densities (OD) = 3.5 at $\lambda_{\text{max}} = 350$ nm, Figure 2A). We hypothesized that thinner films might offer greater sensitivity, as has been shown for polymers that detect TNT,¹⁷ because analytes introduced to the top of the film quench excitons generated within their characteristic diffusion lengths. However, our original synthesis conditions required shorter reaction times (24 or 48 h) to produce thinner films, and these films showed lower stilbene content and inferior sensing performance.

TPV films grown in the presence of allylsilane-functionalized SiO₂ provided access to thinner films that exhibited superior sensitivity and response rates. Film performance was optimized by varying the initial monomer concentration ($[1]_0$) and reaction time. TPV films grown at lower $[1]_0$ (5 mM) exhibited

Received: March 5, 2015

Revised: April 17, 2015

Published: May 5, 2015

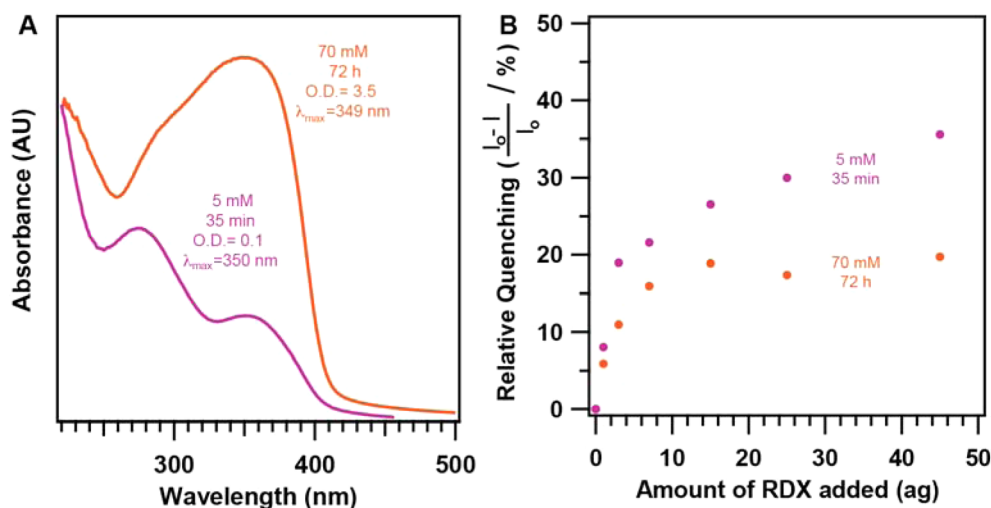


Figure 2. (A) UV/vis absorbance spectra of TPV films grown on allyl silane-functionalized fused SiO_2 at $[1]_0 = 5 \text{ mM}$ for 35 min (purple) and $[1]_0 = 70 \text{ mM}$ for 72 h (orange). The spectra have been normalized to accurately display their features, and the absolute optical density of each film at its lowest-energy λ_{max} (349 or 350 nm) is listed. (B) Fluorescence quenching % of TPV films grown at 5 mM concentration for 35 min (purple) and 70 mM concentration for 72 h (orange) in response to attogram (ag) quantities of RDX.

a similar absorbance trend as a function of reaction time that was observed in thicker films. At shorter reaction times (0.5–2 h), the ratio of optical densities at 350 to 280 nm ($\text{OD}_{350}/\text{OD}_{280}$) was relatively low (0.3–0.5), corresponding to a low extent of reaction and a film with many residual vinyl groups. At longer reaction times (16–72 h), this ratio increased to between 0.9 and 1.1, which is indicative of greater stilbene content (Figure S3 in the Supporting Information). Key differences compared to experiments run at $[1]_0 = 70 \text{ mM}$ are notable: the absolute optical density of the film does not increase at longer reaction times and absorbance peak at 280 nm does not completely disappear. We hypothesize that most of the alkenes in the film have reacted within 16 h, such that the film has few dangling bonds to enable further growth. Alkenes bonded to the nonconjugated allyl silane monolayer also absorb at $\lambda = 280 \text{ nm}$ and represent a higher percentage of the chromophores present when the films are thin. Films grown at reduced $[1]_0$ also exhibited a lower $\text{OD}_{350}/\text{OD}_{280}$ indicating a reduced stilbene content, which is also consistent with our hypothesis that this bond is partially attributable to reactions with the surface-bound allyl groups (Figure S2 in the Supporting Information).

The fluorescence response of TPV films to RDX solution and vapors suggest that stilbene content and film thickness are opposing parameters that affect sensitivity of detection. RDX was extracted from commercially available canine training aids and purified by dissolving RDX in CH_3CN and triturating with CHCl_3 (see safety information in the Supporting Information). This procedure was repeated twice to provide RDX crystals whose only obvious contaminant was $\sim 2\%$ of the explosive HMX, as determined by ^1H NMR spectroscopy. A RDX stock solution (1 mg/mL in CH_3CN) was prepared and diluted further to introduce attogram (ag) quantities of RDX to the TPV film. After the initial fluorescence of a TPV film was recorded, RDX solution was placed on the substrate, and the solvent was removed by evacuation. The fluorescence of the films was remeasured. Despite their lower stilbene content, TPV films grown for 35 min in $[1]_0 = 5 \text{ mM}$ displayed 19% quenching upon addition of 3 ag of RDX and 36% quenching to 85 ag of RDX, which is superior to those grown for 72 h at

$[1]_0 = 70 \text{ mM}$ that exhibited 11% quenching at 3 ag of RDX and 22% quenching at 85 ag of RDX (Figure 2B). The fluorescence of films treated with the same sample of CH_3CN used to prepare the RDX stock solution exhibited no quenching, indicating that this response cannot be attributed to residual solvent or its trace impurities. These results indicate that TPV films grown for 35 min at 5 mM concentration represent a balance between film thickness and stilbene content.

The TPV films provide selective and measurable responses to RDX vapor within a few seconds of exposure time. This effect was characterized using a customized fluorometer that monitors the TPV film fluorescence in real time in the presence of a solid RDX sample (4 mg) suspended approximately 1 cm from the substrate. The fluorescence intensity of a TPV film was recorded every 5 s both in the presence and absence of RDX. The optimized TPV films exhibited $1.6 \pm 0.4\%$ fluorescence quenching at 10 s, which increased to $7.1 \pm 1.3\%$ after 90 s (Figure 3). The continuous irradiation of the TPV films in this instrument also photobleached the sample over time. Therefore, the film's response to RDX vapor was compared to the rate of photobleaching that occurred as a consequence of its continuous photoexcitation. The fluorescence quenching response to RDX vapors is clearly discernible over the photobleaching rate (Figure 3). In contrast, TPV films exposed to CH_3CN vapors over time exhibited an enhancement in fluorescence, which we noted in our previous report (Figures S24 and S25 in the Supporting Information). Again, this control experiment confirms that the fluorescence quenching response observed in TPV films is due to an interaction with RDX vapor and not trace volatile solvent impurities. These experiments demonstrate that RDX vapors are detected within 10–15 s under these conditions. It may prove possible to further shorten this time by optimizing the intensity of the excitation source or designing more photostable polymer networks.

Much like the results obtained for detecting RDX introduced from solution, $[1]_0$ and reaction time strongly influence the fluorescence quenching response of TPV films to RDX vapors. The magnitude of fluorescence quenching doubled from 4% to

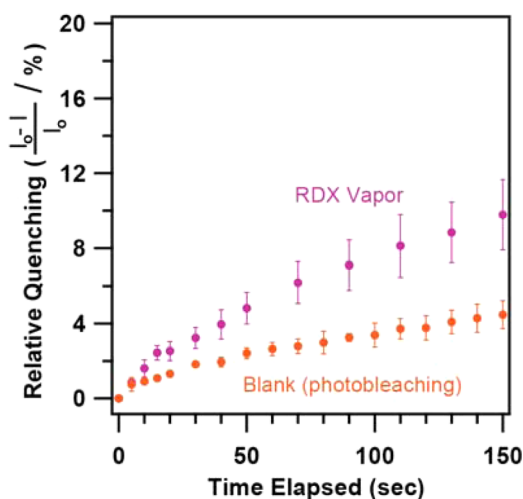


Figure 3. Fluorescence quenching % of TPV film grown at 5 mM concentration for 35 min in response to RDX vapor over time (purple) and due to photobleaching (orange). Each data point indicates the average response of three different films. The error bars show one standard deviation from the average.

8% at 90 s in films grown at $[1]_0 = 5$ mM instead of 3.5 mM (Figure 4A). We attribute this increase in the sensitivity to an increase in stilbene content of the films grown at 5 mM but minimal increase in corresponding film thickness, as characterized by UV/vis spectroscopy. TPV films grown at $[1]_0 = 70$ mM showed only minimal fluorescence quenching response to RDX vapor, which can be attributed to their increased thickness (Figure S2 in the Supporting Information). It is unsurprising that vapor detection performance is even more sensitive to film thickness than experiments performed by introducing RDX from solution because the solvent can distribute the analyte throughout the film whereas RDX vapor first interacts with the top surface of the film. A logical trend was also observed in the fluorescence quenching response of TPV films grown in 5 mM reaction mixture for different time intervals. Longer growth time periods led to improved stilbene content (Figure S3 in the Supporting Information). Concomitantly, improved fluorescence response was observed. TPV films grown for 35 min and

48 h exhibited similar quenching response of 6% and 7%, respectively, after 90 s exposure to RDX vapor (Figure 4B). More precise and consistent response was observed in TPV films grown with $[1]_0 = 5$ mM for 35 min (Figure 3 and Figure S13 in the Supporting Information). However, it should be noted that TPV films grown for 2 and 16 h display distinct but reproducible UV/vis absorbance profiles and reduced fluorescence quenching performance, which underscores the nonlinear relationship between reaction time and sensitivity of detection (Figure 4B and Figure S3 in the Supporting Information). Further studies are needed to understand the evolution of TPV thin-film structure as a function of reaction time.

The fluorescence response of TPV films to RDX vapors differs with the age of RDX crystals, suggesting that the material responds to RDX itself and not its degradation products. RDX has poor photostability and forms a variety of decomposition products when exposed to light, such as hexahydro-1-nitroso-3,5-dinitro-1,3,5-triazine (MNX), hexahydro-1,3,5-trinitroso-1,3,5-triazine (TNX), 1,3-dinitro-1,2,3,4-tetrahydro-1,3,5-triazine (MUX), 1,3,5-triazine (TUX). RDX was crystallized twice, stored at low temperature, and protected from light prior to performing quenching experiments. Previously we reported that TPV films were most sensitive to pure RDX in solution, and we compared to it photodegraded RDX and a 6 month old analytical standard. Similar results were observed upon exposing optimized TPV films to RDX vapors. A relative quenching of 2% was observed on exposure of TPV film to 1 month old RDX while a relative quenching of 0.8% was observed on exposure to TPV film to 1 year old RDX (Figure S15 in the Supporting Information). This further emphasizes the ability to TPV to interact well with RDX molecules in comparison to decomposition products from its photolysis.

Optimized TPV films were employed to detect HMX, a higher molecular weight nitramine explosive. HMX has an equilibrium vapor pressure of ~ 0.01 ppt, more than 2 orders of magnitude lower than RDX (6 ppt). A commercial HMX analytical standard (1 mg/mL) was diluted to deliver attogram quantities of HMX. The optimized TPV films exhibited a fluorescence quenching response of $16 \pm 3\%$ on exposure to 3 ag of HMX, which saturated at $33 \pm 3\%$ at 85 ag (Figure 5).

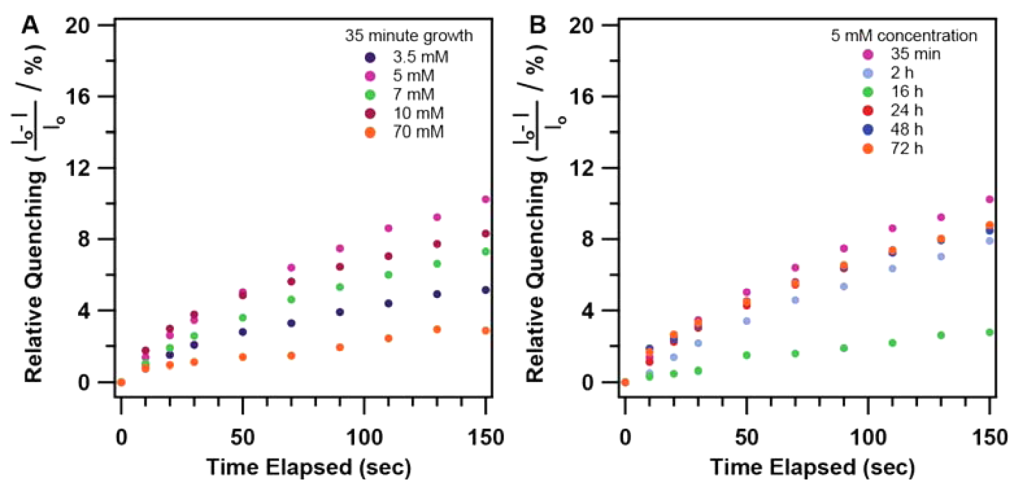


Figure 4. (A) Fluorescence quenching of TPV films grown for 35 min at concentrations of 3.5 mM (blue), 5 mM (purple), 7 mM (green), 10 mM (red), and 70 mM (orange). (B) Fluorescence quenching % of TPV films grown for at 5 mM concentration for 35 min (purple), 2 h (blue), 16 h (green), 24 h (red), 48 h (blue), and 72 h (orange). Each data point indicates the average response of three different films.

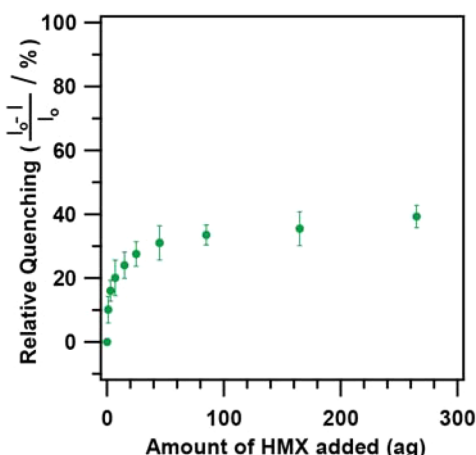


Figure 5. Fluorescence quenching % of TPV films grown at $[1]_0 = 5$ mM for 35 min in response to attograms of an HMX solution in CH_3CN . Each data point indicates the average response of three different films. The error bars show one standard deviation from the average.

However, TPV films do not show any quenching when exposed to HMX vapors under identical conditions to those used for RDX (Figure S27 in the Supporting Information), presumably because of HMX's lower volatility. It should also be noted that our commercial HMX analytical standard contained a 0.002% RDX impurity. Because of the lack of availability of a pure HMX sample, we cannot rigorously disprove that this impurity contributes to the fluorescence quenching response on exposure to attogram quantities of HMX solution. However, this prospect is unlikely because ag quantities of HMX containing RDX impurities deliver extremely low quantities of RDX (1×10^{-23} g) that fall outside the detection limits of the TPV films. The TPV films also respond to 2,4-dinitrotoluene vapors (Figures S21 and 22 in the Supporting Information), albeit with inferior performance to other systems.¹⁶

In conclusion, we achieved improved control of the growth of TPV films by employing an allyl-functionalized substrate in the reaction mixture. This advance provided access to thin films that exhibited increased sensitivity and faster response to RDX introduced from solution ($\sim 2\text{--}3$ ag) and from the vapor phase (as low as 10 s). The optimized films also detected HMX introduced from solution (~ 3 ag) but its even lower volatility precluded vapor detection. The extraordinary sensitivity of these polymer films appears to depend on both their thickness and extent of conjugation imparted by the alkene metathesis reaction. Furthermore, this advance should enable TPV and other alkene-containing polymer networks to be bonded to arbitrary surfaces, such as the interior walls of capillaries that would otherwise be difficult to coat with an insoluble, cross-linked polymeric solid. These findings are of interest for security applications and demonstrate the potential of conjugated polymer networks to detect analytes of interest.

■ ASSOCIATED CONTENT

⑤ Supporting Information

Experimental procedures and fluorescence response of TPV films to explosives is in the SI. The Supporting Information is available free of charge on the ACS Publications website at DOI: 10.1021/acs.chemmater.5b00857.

■ AUTHOR INFORMATION

Corresponding Author

*E-mail: wdichtel@cornell.edu.

Funding

This research was supported by the NSF CAREER award (CHE-1056657). We also made use of the Cornell Center for Materials Research Shared Facilities, which are supported through the NSF MRSEC program (DMR-1120296). D.G. acknowledges the award of a Faculty for the Future fellowship from the Schlumberger Foundation.

Notes

The authors declare no competing financial interest.

■ ACKNOWLEDGMENTS

We thank Smiths Detection, especially Dr. Reno DeBono, for helpful discussions and the loan of the fluorometer used for real-time quenching experiments.

■ REFERENCES

- (1) Charles, P. T.; Kusterbeck, A. W. *Biosens. Bioelectron.* **1999**, *14*, 387.
- (2) Desmet, C.; Blum, L. J.; Marquette, C. A. *Anal. Chem.* **2012**, *84*, 10267.
- (3) Moros, J.; Laserna, J. J. *Anal. Chem.* **2011**, *83*, 6275.
- (4) Farrell, M. E.; Holthoff, E. L.; Pellegrino, P. M. *Proc. SPIE* **2012**, 8358, 835816/1.
- (5) Tabrizchi, M.; Ilbeigi, V. *J. Hazard. Mater.* **2010**, *176*, 692.
- (6) Riskin, M.; Tel-Vered, R.; Willner, I. *Adv. Mater.* **2010**, *22*, 1387.
- (7) Ja, S.-J. *Proc. SPIE* **2012**, 8358, 83580S/1.
- (8) Xiong, R.; Odbadrakh, K.; Michalkova, A.; Luna, J. P.; Petrova, T.; Keffer, D. J.; Nicholson, D. M.; Fuentes-Cabrera, M. A.; Lewis, J. P.; Leszczynski, J. *Sens. Actuators, B* **2010**, *B148*, 459.
- (9) Andrew, T. L.; Swager, T. M. *J. Am. Chem. Soc.* **2007**, *129*, 7254.
- (10) Andrew, T. L.; Swager, T. M. *J. Org. Chem.* **2011**, *76*, 2976.
- (11) Blake, T.; Kelly, J.; Gallagher, N.; Gassman, P.; Johnson, T. *Anal. Bioanal. Chem.* **2009**, *395*, 337.
- (12) Brudzewski, K.; Osowski, S.; Pawlowski, W. *Sens. Actuators, B* **2012**, *161*, 528.
- (13) Cabalo, J.; Sausa, R. *Appl. Spectrosc.* **2003**, *57*, 1196.
- (14) Freeman, R.; Willner, I. *Nano Lett.* **2009**, *9*, 322.
- (15) Li, X.; Li, Q.; Zhou, H.; Hao, H.; Wang, T.; Zhao, S.; Lu, Y.; Huang, G. *Anal. Chim. Acta* **2012**, *751*, 112.
- (16) Thomas, S. W.; Joly, G. D.; Swager, T. M. *Chem. Rev.* **2007**, *107*, 1339.
- (17) Yang, J.-S.; Swager, T. M. *J. Am. Chem. Soc.* **1998**, *120*, 11864.
- (18) Freeman, R.; Finder, T.; Bahshi, L.; Gill, R.; Willner, I. *Adv. Mater.* **2012**, *24*, 6416.
- (19) Hu, Z.; Tan, K.; Lustig, W. P.; Wang, H.; Zhao, Y.; Zheng, C.; Banerjee, D.; Emge, T. J.; Chabal, Y. J.; Li, J. *Chem. Sci.* **2014**, *5*, 4873.
- (20) Lan, A.; Li, K.; Wu, H.; Kong, L.; Nijem, N.; Olson, D. H.; Emge, T. J.; Chabal, Y. J.; Langreth, D. C.; Hong, M. *Inorg. Chem.* **2009**, *48*, 7165.
- (21) Lan, A.; Li, K.; Wu, H.; Olson, D. H.; Emge, T. J.; Ki, W.; Hong, M.; Li, J. *Angew. Chem., Int. Ed.* **2009**, *48*, 2334.
- (22) Liu, X.; Xu, Y.; Jiang, D. *J. Am. Chem. Soc.* **2012**, *134*, 8738.
- (23) Che, Y.; Gross, D. E.; Huang, H.; Yang, D.; Yang, X.; Discekici, E.; Xue, Z.; Zhao, H.; Moore, J. S.; Zang, L. *J. Am. Chem. Soc.* **2012**, *134*, 4978.
- (24) Gopalakrishnan, D.; Dichtel, W. R. *J. Am. Chem. Soc.* **2013**, *135*, 8357.
- (25) Wang, Y.; La, A.; Ding, Y.; Liu, Y.; Lei, Y. *Adv. Funct. Mater.* **2012**, *22*, 3547.